

# Curing Behavior of Ceramic Resin for Stereolithography

G. Allen Brady, Tien-Min Chu and John W. Halloran  
Materials Science and Engineering Department, College of Engineering  
The University of Michigan, Ann Arbor, MI. 48109

## ABSTRACT

Ceramic green bodies have been created with stereolithography methods by using ultraviolet curable suspension of ceramic powders, a "ceramic resin", on a Stereolithography Apparatus (SLA). A minivat system with mini-recoater blade was designed to run small batch experiments on an SLA-250/40 machine. With the ceramic resins developed from hydroxyapatite for biomedical application and from alumina and silica for making metal casting molds, ceramic green bodies were built. Diagnostic parts of these ceramic resins were made with the Accumax diagnostic kit (3D Systems) and the curing parameters determined. The effect of shrinkage stress and scattering will be discussed.

## Introduction

Since the early 1990's, the Stereolithography (SL) technique has been the predominant fabrication method for rapid prototyping[1]. The SL technique involves solidification of a liquid resin by a UV-laser source. The laser cures one layer by "drawing" it on the surface of a vat of resin. The 3-dimensional part is built layer by layer. The research at the University of Michigan is focused on developing new materials, particularly ceramic materials, for use in a Stereolithography Apparatus (SLA)<sup>a</sup>. These ceramic resins are used in the same manner as the traditional epoxy or acrylate resins. However, instead of producing a 100% polymer part, these ceramic resins yield a ceramic green body consisting of approximately 50% ceramic and 50% uv-polymerized binder. Current materials include alumina, silica and hydroxyapatite (HA). Potential applications for the alumina and silica resins include cores and shell molds for investment casting as well as functional ceramic prototypes. HA ceramics have significant biomedical applications[2,3].

These ceramic resins are fluid suspensions of ceramic particles in a uv-curable medium. For ceramic processing purposes, the resins must be highly loaded (at least 50 volume%) to produce reliable, dense finished ceramic parts. For SL processing purposes, the resins must have a low viscosity (< 5000 cps) to undergo the recoating process<sup>b</sup>, and self-leveling.

The cure depth is defined in the "Working Curve" equation,

$$C_d = D_p \ln \frac{E}{E_c} \quad (1)$$

where  $E$  is the average exposure dose supplied by the laser (controlled by scanning speed,  $v_s$ ),  $C_d$  is the user definable cure depth and  $D_p$  and  $E_c$  are resin parameters respectively known as depth

---

a. Model SLA250/40, 3D Systems, Valencia, CA.

b. Recoating here refers to the doctor-blade type of recoating found on SLA 250

of penetration and critical exposure. A schematic of resin curing under a laser is shown in Figure 1. While intensity attenuation for traditional resins used for SL is limited by absorption, the intensity decrease of the uv-radiation in these turbid suspensions is controlled by scattering. The following relation has been used to describe the effect of scattering on cure depth[3,5],

$$C_d = \left( \frac{2}{3} \cdot \frac{d}{\phi \beta \Delta n^2} \right) \ln \frac{E}{E_c} \quad (2)$$

where  $\phi$  is the volume fraction solids,  $d$  is the particle size and  $\Delta n$  is the difference in index of refraction between the suspended particles (ceramic) and medium (photocurable monomer resin). The  $\beta$  term involves interparticle spacing and wavelength of radiation.

### Materials and Methods

Three resins systems are examined in this work, alumina-aqueous, silica-acrylate and hydroxyapatite-acrylate. Details of resin fabrication are given elsewhere[3]. The alumina-aqueous resin is 52vol% solids with a monomer solution consisting<sup>c</sup> of 27% N-hydroxymethacrylamide, 3% methylene bis-acrylamide, 35% water and 35% ethylene glycol. The silica-acrylate resin has 43vol% solids, and the monomer solution is 30% 2-ethoxyethoxy ethyl acrylate and 70% hexane diol diacrylate. The HA-acrylate resin has 40vol% solids and the monomer solution is 66% octyl-decyl acrylate, 22% hexane diol diacrylate and 12% trimethylolpropane triacrylate.

All parts were produced on an SLA 250/40 with a He/Cd laser source. Typically, the laser power at the surface of the resin was about 30 mW. The machine was equipped with an exchangeable minivat (1L to 2L) with a recoating arm (shown in Figure 2) for small sample experiments. Some single layer parts were produced in a glass petri dish on an adjustable stand rather than the minivat. The Windowpane technique[1] was used to measure the cure depth as a function of exposure from which the resin parameters,  $D_p$  and  $E_c$  were determined for each resin. After curing in the SLA-250, parts were postcured 30 minutes in a uv chamber and allowed to dry at ambient temperature. To remove the photopolymers from the postcured parts, a burnout was performed in air. The parts were heated slowly (1°C/min) to 500°C, held 1 hour, then cooled. To sinter the alumina parts, they were heated in air to 1550°C (10°C/min), held 1 hour then cooled.

### Results

The cure depth as a function of energy dose is plotted in Figure 3 for the ceramic resins and the standard epoxy resin. In each case, the cure depth is linear with  $\ln(E)$ , although the slopes( $D_p$ ) do differ widely. The resin parameters were determined from these data and are listed in Table 1. In each case, the linear relation between the cure depth and  $\ln(\text{energy dose})$  is apparent. The effect of these resin parameters are shown qualitatively in the cured line profiles shown in Figure 4 for silica and alumina. As the  $D_p$  decreases, the cured profile becomes wider and more shallow. A "Block M" shape was made in alumina and HA and also in SL 5170 for comparison. An epoxy M, an alumina M after post-curing and an alumina M after sintering are shown in Figure 5 (from right to left respectively). From this photo, curing and drying shrinkage of the alumina-aqueous resin is not much larger than that of the SL 5170. The significant portion of shrinkage occurred in the sin-

---

c. all percentages are given in weight percent unless otherwise noted.

tering step, approximately 12% (linear). No cracking or significant warping occurred during either curing, drying, or sintering. A fracture surface of one section of the alumina M is shown in Figure 6. The image to the left shows a scalloped edge resulting from the wide, shallow shape of the cured line profile. At higher magnification in the right image, the interface between two layers appears to have sintered very well with no remnants of the layered processing evident.

**Table 1. Resin Parameters**

Resin	$D_p$ , $\mu\text{m}$	$E_c$ , $\text{mJ}/\text{cm}^2$
Cibatool® SL-5170	119	10.2
$\text{Al}_2\text{O}_3$ -Aqueous	69	19.4
$\text{SiO}_2$ -Acrylate	260	13.4
HA-Acrylate	56	10.8

A portion of a the Block M shape built from HA-acrylate is shown in Figure 7. The side surface also has a scalloped appearance, but the layers appeared to be knit together well. However, shrinkage cracking occurs during curing and is shown in Figure 8 to occur between the borders on the layers.

## Discussion

All resins used in this work follow a predictable relation between cure depth and energy dose. Work is continuing to increase the stiffness and solids loading of these ceramic resins. Layer cure depths of 200  $\mu\text{m}$  to 600  $\mu\text{m}$  are achievable with the silica resin, 180  $\mu\text{m}$  to 300  $\mu\text{m}$  for the alumina resin and 200  $\mu\text{m}$  to 300  $\mu\text{m}$  for the HA resin. Parts have been built with adequate layering. The microstructure of a part fabricated in the alumina resin reveals no remnants of layered processing.

Side scattering produces the scalloped edges found on some initial parts built at Michigan. A side view of several cured lines drawn one upon another are shown in Figure 9 which illustrates the scalloping effect. The phenomenon also occurs in alumina-aqueous resins. The refractive index difference ( $\Delta n^2$ ) in the alumina-aqueous is approximately 0.076. Reducing  $\Delta n^2$  by using an acrylate-based solution ( $n= 1.447$  vs. 1.425 for aqueous solution) would reduce  $\Delta n^2$  to 0.064, subsequently decreasing the level side-scattering while increasing the cure depth.

Shrinkage cracking occurred in the acrylate resin systems (with both silica and HA). This cracking did not occur in the alumina-acrylate system which only experienced minor shrinkage (<3% linear). There are two simple ways to alleviate these shrinkage stresses. One is to employ an unreactive diluent in the acrylate solution. This decreases the concentration of the acrylate bonds in the resin and thus the curing shrinkage. For example, in the alumina-aqueous system, water and ethylene glycol are unreactive diluents which dry after curing. The second method is to make use of new build styles. Build style refers to the algorithms used to generate the path of the laser when drawing each layer. The power of optimizing the build style to control shrinkage is seen

in the use of SL5170 epoxy resin with the ACES™ build style. The theoretical shrinkage is 6.2%, but use of this build style manages the shrinkage to an effective 0.05% in the x and y directions! Experimentation on build styles for the specific ceramic resins is currently underway.

Scattering contributes to lower depths of penetration by the uv-radiation as well as to larger line widths. The overall shapes of the line profiles are more shallow than in the unfilled resin also due to scattering. As a result, more radiation is delivered in a sideways direction which increases the line width. In order to build accurate parts, this increased line width must be dealt with in the build style. Work is underway to characterize and model the shape of the cured line profile for these resins. Despite the progress made to date on elementary fabrication, shrinkage issues and the effect of scattering emphasizes the need to fully exploit the capabilities of the SLA-250 by creating new build styles to both accommodate the modified line profile and alleviate shrinkage and distortion.

### **Acknowledgment**

The research on the refractory ceramics is supported by the Office of Naval Research under contracts N00014-95-1-0527 through Dr. S. Fishman and R. Wachter and the research on bioceramics is supported through the University of Michigan by a Rackham Grant to T-M. Chu.

### **References**

1. P. F. Jacobs, Rapid Prototyping & Manufacturing-Fundamentals of Stereolithography, 1st ed., Society of Manufacturing Engineers, Dearborn, MI (1992).
2. G. de Lange, "The Bone-Hydroxyapatite Interface", pp. 61-75 in *Handbook of Bioactive Ceramics*, Vol. 4, (eds.) T. Yamamuro, L. L. Hench and J. Wilson, CRC Press, Inc., Boca Raton, FL, 1990.
3. C. A. van Blitterswijk, J. J. Grote, W. Kuijpers, W. T. Daems and K. de Groot, "Macropore Tissue Ingrowth: A Quantitative and Qualitative Study on Hydroxyapatite Ceramic", *Biomaterials*, **7** 137-143 (1986).
4. M. L. Griffith, "Stereolithography of Ceramics", Ph.D. Thesis, University of Michigan, March, 1995.
5. M. L. Griffith and J. W. Halloran, "Free Form Fabrication of Ceramics by Stereolithography", submitted to *Journal of the American Ceramic Society*.

## FIGURES

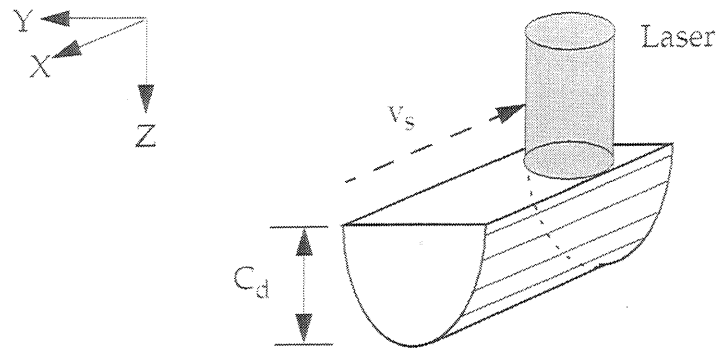


Figure 1 Schematic of a cured line profile generated by laser scanning on the resin surface.

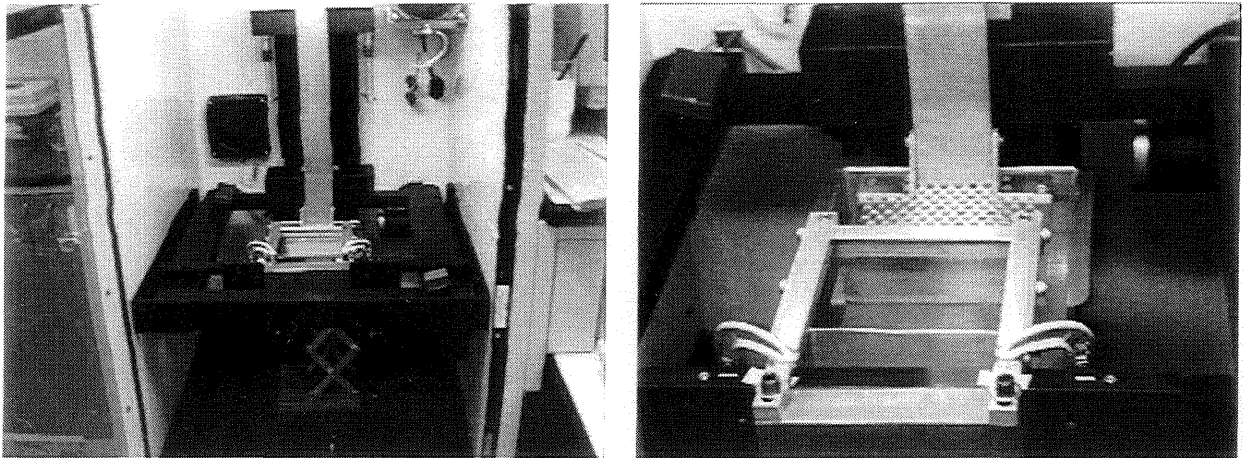


Figure 2 Photos of exchangeable minivat system. Elevator platform and recoating blade are shown at the right.

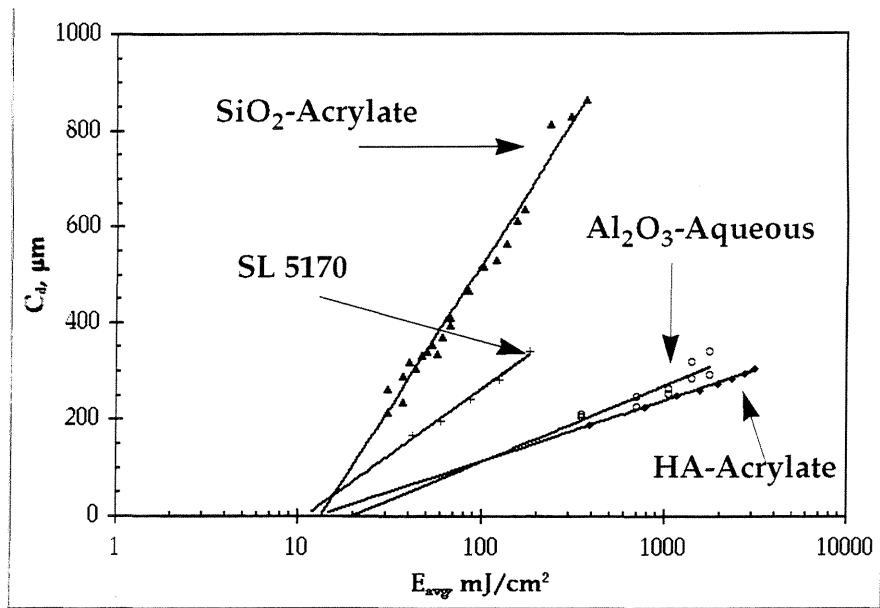


Figure 3 Working curves for silica-acrylate, alumina-aqueous, HA-acrylate resins.

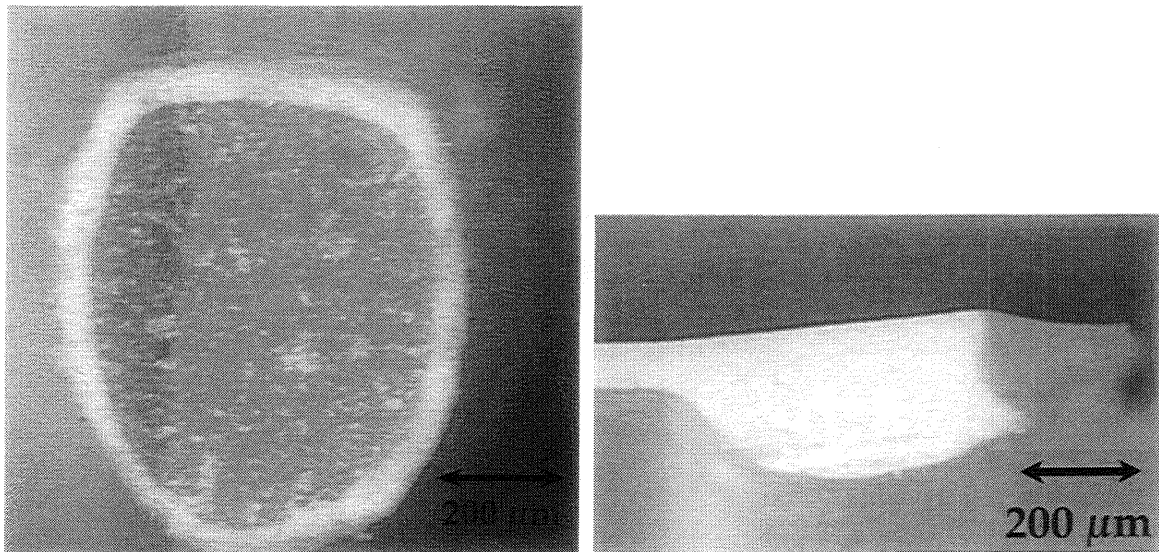


Figure 4 Cured line profile for silica-acrylate resin (left) and alumina-aqueous (right).

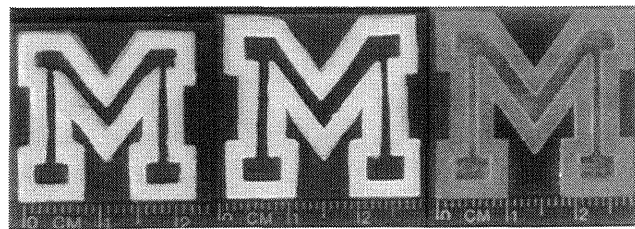
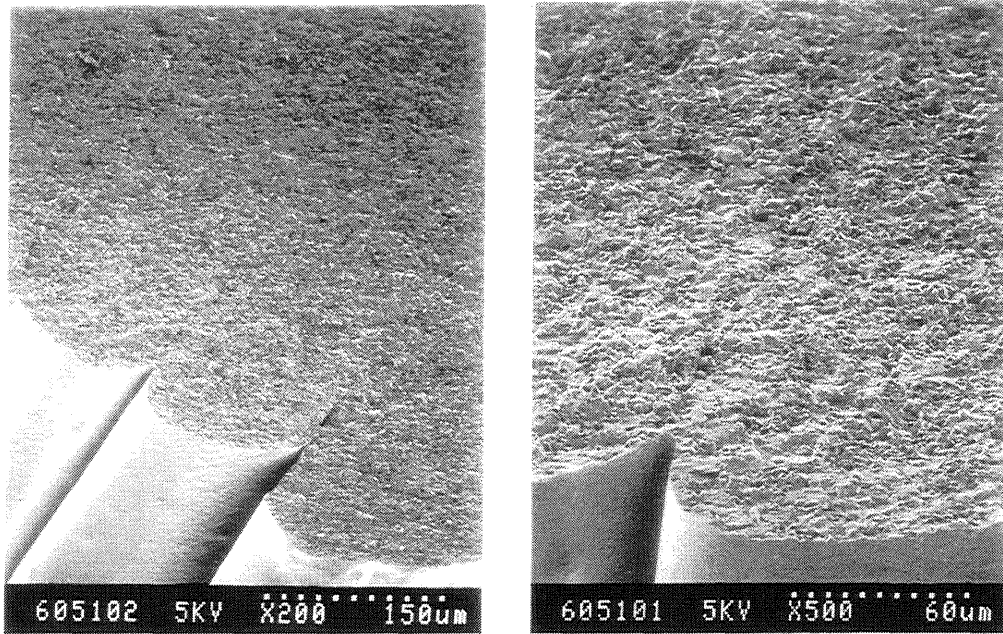
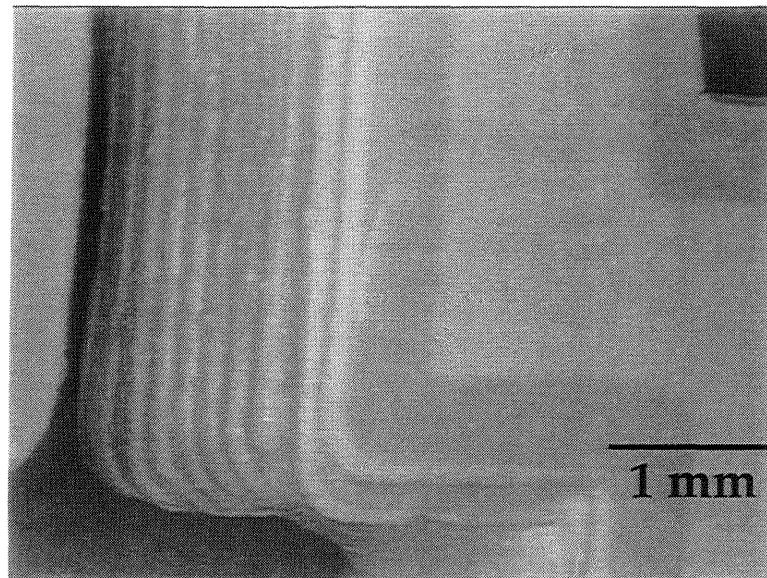


Figure 5 Block M's: epoxy on the right, alumina-as cured in the center and alumina-after sintering at  $1550^{\circ}C$  for 1 hour.



**Figure 6** Fracture surface of sintered alumina “Block M” made from alumina-aqueous resin. Note scalloped edges on left. Close-up picture on the right shows no evidence of layering.



**Figure 7** Tilted view of HA-acrylate “M” showing scalloped edges. Note contrast between border and fill regions.



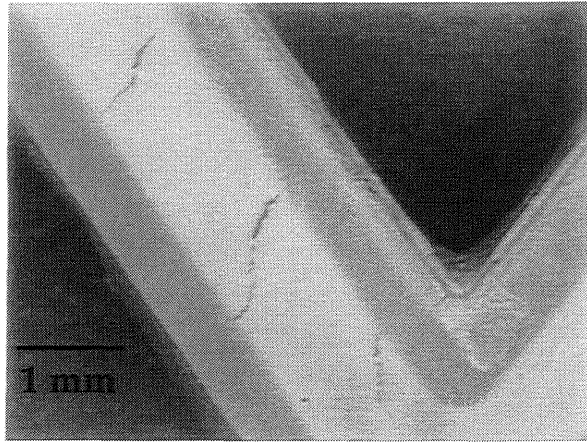


**Figure 8** Shrinkage cracks in HA-acrylate between borders.

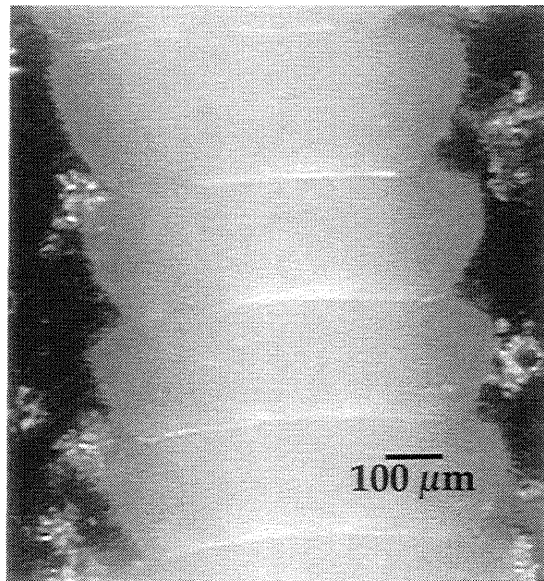


**Figure 9** Stacking of cured profiles in HA-acrylate resin.